Bioresource Technology 293 (2019) 122067

Contents lists available at ScienceDirect

Bioresource Technology

journal homepage: www.elsevier.com/locate/biortech

Application of phase-pure nickel phosphide nanoparticles as cathode catalysts for hydrogen production in microbial electrolysis cells

Kyoung-Yeol Kim[a,c,*], Susan E. Habas[b], Joshua A. Schaidle[b], Bruce E. Logan[c]

[a] Department of Environmental and Sustainable Engineering, University at Albany, State University of New York, 1400 Washington Avenue, Albany, NY 12222, United States

[b] National Bioenergy Center, National Renewable Energy Laboratory, Golden, CO 80401, United States

[c] Department of Civil and Environmental Engineering, The Pennsylvania State University, 231Q Sackett Building, University Park, PA 16802, United States

GRAPHICAL ABSTRACT

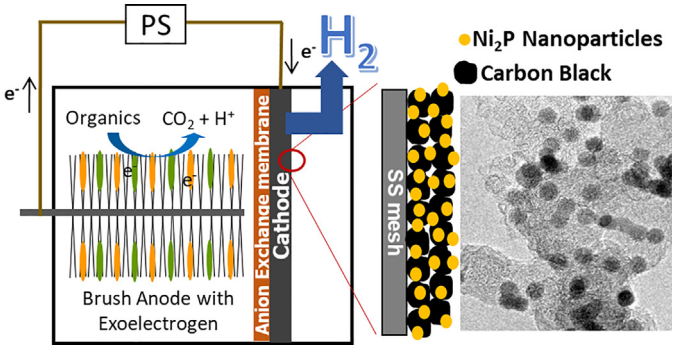

ARTICLE INFO

Keywords:
Phase-pure metal phosphide nanoparticles
Microbial electrolysis cell
Hydrogen evolution reaction
Non-precious metal catalysts
Fermentation effluent

ABSTRACT

Transition metal phosphide catalysts such as nickel phosphide (Ni_2P) have shown excellent activities for the hydrogen evolution reaction, but they have primarily been studied in strongly acidic or alkaline electrolytes. In microbial electrolysis cells (MECs), however, the electrolyte is usually a neutral pH to support the bacteria. Carbon-supported phase-pure Ni_2P nanoparticle catalysts (Ni_2P/C) were synthesized using solution-phase methods and their performance was compared to Pt/C and Ni/C catalysts in MECs. The Ni_2P/C produced a similar quantity of hydrogen over a 24 h cycle (0.29 ± 0.04 L-H_2/L-reactor) as that obtained using Pt/C (0.32 ± 0.03 L-H_2/L) or Ni/C (0.29 ± 0.02 L-H_2/L). The mass normalized current density of the Ni_2P/C was 14 times higher than that of the Ni/C, and the Ni_2P/C exhibited stable performance over 11 days. Ni_2P/C may therefore be a useful alternative to Pt/C or other Ni-based catalysts in MECs due to its chemical stability over time.

1. Introduction

Microbial electrolysis cells (MECs) can produce hydrogen gas from organic matter in wastewater using exoelectrogenic microorganisms on the anode (Lu and Ren, 2016). These microorganisms can oxidize organic matter and transfer electrons to the electrode surface, where the

* Corresponding author at: Department of Environmental and Sustainable Engineering, University at Albany, State University of New York, 1400 Washington Avenue, Albany, NY 12222, United States.
E-mail address: kkim28@albany.edu (K.-Y. Kim).

https://doi.org/10.1016/j.biortech.2019.122067
Received 2 June 2019; Received in revised form 19 August 2019; Accepted 24 August 2019
Available online 27 August 2019
0960-8524/

electrons are transferred through the circuit to drive (with additional voltage applied) the hydrogen evolution reaction (HER, $2H^+ + 2e^- \rightarrow H_2$) on the cathode (Rozendal et al., 2006). The cathode catalyst is crucial to the performance of the MEC as it affects hydrogen production rates and capital costs. Platinum (Pt) catalysts have been widely used in lab-scale MECs due to their excellent catalytic activities for HER. However, the use of this expensive precious metal catalyst is not economical (Rozendal et al., 2008). Thus, it is important to develop inexpensive but highly efficient and stable cathode catalysts to replace Pt for practical MEC applications.

Various non-precious metal catalysts, such as nickel (plates, foams and adsorbed Ni on activated carbon), MoS_2, and stainless steel, have been tested as alternatives to Pt in MECs (Call et al., 2009; Hrapovic et al., 2010; Kim et al., 2018; Lu et al., 2016; Tokash and Logan, 2011). Nickel has the advantages of being a relatively earth-abundant metal that exhibits high catalytic activity for HER due to weak atomic hydrogen binding as determined from density functional theory (DFT) calculations (Nørskov et al., 2005), and its performance is similar to that of Pt in MEC tests. For example, MECs with Ni powder cathodes produced 1.2 L-H_2 per day per liter of reactor volume (L-H_2/L-d), which was comparable to that obtained with a Pt catalyst (Selembo et al., 2010). Similar rates were also obtained using nickel salts adsorbed onto activated carbon (Kim et al., 2018). In a highly optimized reactor with very thin chambers, MECs with a Ni foam cathode initially produced a much higher rate of 50 L-H_2/L-d, but this rate decreased over time (Jeremiasse et al., 2010). Although nickel catalysts can have comparable catalytic activities to Pt in MECs, pure nickel is unstable and prone to corrosion (Selembo et al., 2010).

Recently, transition metal phosphides have been demonstrated to exhibit improved stability and catalytic activity for HER as compared to transition metal catalysts (Shi and Zhang, 2016; Xiao et al., 2015), in some cases with conversion efficiencies on par with Pt (Laursen et al., 2015). Nickel phosphide (Ni_2P), for example, showed a variation in overpotential of < 25 mV after 500 cyclic voltammetric (CV) sweeps in 0.5 M H_2SO_4 (Popczun et al., 2013). A previous study attributed the excellent catalytic activity of Ni_2P to the negatively charged phosphorus atom that can attract more positively charged protons and reduce the hydrogen binding energy (Liu and Rodriguez, 2005). Ni_2P catalysts have been primarily tested in strongly acidic or alkaline electrolytes in water electrolyzers (Feng et al., 2014; Popczun et al., 2013; Wu et al., 2018; Zhou et al., 2016). However, only a few studies have evaluated Ni_2P catalysts under near-neutral pH conditions (Han et al., 2015; Shi et al., 2015; Sun et al., 2017; Zhang et al., 2017). Operation under neutral to mildly alkaline conditions at the cathode is necessary for MECs. Thus far, nickel phosphide catalysts have only been examined for their use in MECs in two studies, where different materials were used that were both deposited onto Ni foam: a Ni_5P_4-NiP_2 nanosheet matrix that was synthesized through an energy-intensive combustion process (Cai et al., 2018); or direct chemical plating of a Ni-P coating (Li et al., 2017). In contrast to the mixed phase catalysts prepared by these methods, here we focus on the evaluation of phase-pure, highly monodisperse Ni_2P nanoparticles supported on carbon. While a current density of 14 A/m^2 (the highest value over the 72 h cycle normalized to projected cathode surface area, 2 cm^2) was reported by Cai et al. (2018), the volumetric rate of hydrogen production was not assessed and the impact of the support material (nickel foam) was not examined. Also, it has been shown that surface structure, elemental stoichiometry and corresponding crystal phase, and particle size can impact HER performance of nickel phosphides (Laursen et al., 2015; Pan et al., 2015; Popczun et al., 2013; Seo et al., 2016; Zhou et al., 2016). Therefore, independent control over these physical features is needed to better understand their impact on the performance of nickel phosphide catalysts in MECs. Solution synthesis routes to nanoscale metal phosphides have enabled the correlation of controlled physical properties with catalytic performance, making these materials ideal candidates for integration into electrocatalytic systems (Feng et al., 2014; Popczun et al., 2013).

In order to further examine the potential utility of nickel phosphide catalysts under near-neutral pH conditions relevant to MECs, phase-pure hexagonal Ni_2P nanoparticles (NPs) were synthesized using a solution synthesis method and adsorbed onto high surface area carbon black. In contrast to the mixed phase catalysts prepared in previous studies, this new approach enabled us to synthesize the Ni_2P NPs in a controllable manner and disperse them onto high surface area carbon black, resulting in greater ability to tune performance by modifying nanoparticle size and total loading on the carbon. The performance of this new material was examined in abiotic electrochemical reactors and MECs relative to control cathodes prepared using Pt (Pt/C) or Ni (Ni/C) on activated carbon. The adsorption of the Ni_2P NPs onto carbon black avoided the need for a combustion-based or chemical plating process used in a previous MEC cathode preparation (Cai et al., 2018; Li et al., 2017). Catalytic activities of Ni_2P/C electrodes for HER were evaluated using chronopotentiometry in abiotic tests at neutral and acidic pHs to probe the effect of pH on performance. For MEC tests, the cathode performance was quantified in terms of average current density, net hydrogen production rate, cathodic hydrogen recovery, and energy yield over multiple fed-batch cycles using a synthetic fermentation effluent.

2. Materials and methods

2.1. Synthesis of nickel phosphide nanoparticles on carbon

Ni_2P NPs were synthesized based on a previously described procedure (Habas et al., 2015). Briefly, a mixture of $Ni(PPh_3)_2(CO)_2$ (0.639 g, 1.0 mmol), PPh_3 (1.049 g, 4.0 mmol), dried oleylamine (6.5 mL, 19.9 mmol), and dried 1-octadecene (6.5 mL) were heated under N_2 to 250 °C at ca. 10 °C/min and held for 15 min. The mixture was then heated to 300 °C at ca. 10 °C/min and maintained at 300 °C for 1 h, before removing the heat source and allowing the mixture to cool to room temperature. The resulting NPs were recovered in $CHCl_3$ (ca. 0.5 mL), flocculated with isopropanol (ca. 65 mL), and separated by centrifugation at 8000 rpm for 10 min. The recovered NPs were washed in $CHCl_3$ (ca. 0.5 mL), flocculated with isopropanol (ca. 65 mL), separated by centrifugation and re-dispersed in $CHCl_3$ (ca. 10 mL). The carbon supported Ni_2P NP catalyst was prepared by adding the suspension of NPs dropwise to a rapidly stirring suspension of Vulcan XC-72R (Cabot) in $CHCl_3$ (40 mL) to yield Ni_2P/C with a nominal loading of 20 wt% Ni_2P. The mixture was sonicated for 5 min, stirred overnight, and recovered by centrifugation at x8000 rpm for 10 min. The resulting material was dried under vacuum overnight and then reduced by heating to 450 °C at 5 °C/min in flowing 5% H_2/N_2 (500 sccm) and then holding at 450 °C in the flowing gas mixture for 2 h. After cooling to room temperature, the sample was passivated for 2 h in flowing 1% O_2/N_2 (500 sccm). The reduced Ni_2P/C was briefly exposed to atmosphere and then stored in an N_2-filled glovebox. Prior to catalytic evaluation, the reduced Ni_2P/C was sealed under N_2 and only exposed to air for electrode fabrication.

2.2. Cathode fabrication

Ni_2P/C cathodes were prepared with 2.5 mg-reduced Ni_2P/C per cm^2 (0.5 mg-Ni_2P/cm^2, 20.1 wt% Ni_2P on carbon black, Vulcan XC-72R) onto a stainless steel (SS) mesh (projected surface: 6.5 cm^2, 50 × 50, type 304, McMaster-Carr, USA) current collector using a Nafion binder (5 wt% solution, Aldrich Nafion perfluorinated ion-exchange resin). Pt/C cathodes were prepared with 5.0 mg-Pt/C per cm^2 (0.5 mg-Pt/cm^2, 10 wt% Pt on carbon black, Vulcan XC-72) as a control, following the same procedures described above to fabricate the Ni_2P cathodes (Ribot-Llobet et al., 2013). Ni/C cathodes were also prepared by adsorbing Ni (salt form) onto the activated carbon (6 mg-Ni/cm^2, 18.5 wt% adsorbed Ni on activated carbon, Norit SX Plus), as previously

described (Kim et al., 2018). The Ni/C cathodes were fabricated by a phase inversion technique using a poly(vinylidene fluoride) (PVDF) as a binder, and then immersed into the 1 M $NiCl_2$ solution for adsorption of Ni salts onto the carbon. A greater quantity of metal catalyst was loaded onto the Ni/C cathodes (6 mg/cm^2) relative to the Ni_2P/C and Pt/C cathodes (0.5 mg/cm^2). This was done to enable benchmarking of the cathodes to a commercial Ni foam, which demonstrated a comparable hydrogen production rate to the Ni/C cathode (6 mg/cm^2) in a previous study (Kim et al., 2018).

2.3. Reactor construction and operation

The MECs were made from two polycarbonate cubes that had cylindrical chambers (3 cm in diameter, and 4 cm long, 28 mL in volume for each chamber) that formed the anode and cathode chambers of the MECs. To collect gas from the cathode chamber, a glass tube (diameter of 7.5 cm and a length of 1.5 cm) was attached to the top of the cathode chamber. This tube was sealed using a thick butyl rubber stopper and connected to a gas collection bag (100 mL, Calibrated Instruments, NY) as previously described (Zikmund et al., 2018). The graphite brush anode (2.5 cm diameter, 2.5 cm long; Mill-Rose, Mentor, OH) was first heat treated (450 °C for 30 min) before being used in tests (Feng et al., 2010). The anode and cathode chambers were separated by an anion exchange membrane (AEM, Selemion AMV, AGC Engineering Co. Ltd., JP). The cathodes (Ni_2P/C, Ni/C, or Pt/C cathodes) were placed directly against the AEM, and connected to the circuit using a titanium wire as previously described (Kim and Logan, 2019). Anodes were adopted from microbial fuel cells (MFCs) that have been acclimated over 6 months, and also previously used for 40 days in other MEC tests (Kim et al., 2018).

The solution used in the anode chamber was a synthetic fermentation effluent containing (per liter) as previously described (Kim and Logan, 2019): glucose (0.15 g), sodium acetate (0.27 g), ethanol (0.11 g), lactic acid (0.07 g), and bovine serum albumin (BSA, 0.32 g), in a 50 mM phosphate buffer solution (PBS) containing Na_2HPO_4 (4.58 g), NaH_2PO_4 (3.13 g), NH_4Cl (0.31 g), KCl (0.13 g) in 1 L of DI water, along with a vitamin and mineral solutions. The catholyte contained only 50 mM PBS. Prior to each cycle, the catholyte was sparged with high purity nitrogen gas (99.998%) for 5 min to remove dissolved oxygen. In order to be consistent with previous MEC tests, external voltage was applied using a power supply (BK Precision, USA) at 0.9 V for cycle time of ~24 h (Kim et al., 2017). Both electrolyte solutions were completely replaced with fresh solutions at the start of each cycle. To monitor current, the voltage was measured across a 10 Ω resister every 10 min using a multimeter (Model 2700, Keithley Instruments, Inc., OH) to monitor current.

2.4. Analytical methods and calculations

Powder X-ray diffraction (XRD) data on the Ni_2P materials were collected using a Rigaku Ultima IV diffractometer with a Cu Kα source (40 kV, 44 mA). Diffraction patterns were collected in the 2θ range of 10–100° at a scan rate of 4°/min. The unsupported NPs were drop-cast onto a glass slide from a chloroform suspension. Powder samples (10–20 mg) were supported on a glass sample holder with a 0.5 mm recessed sample area and were pressed into the recession with a glass slide to obtain a uniform z-axis height. The resulting pattern was compared to powder diffraction file (PDF) 01-089-2742 for hexagonal Ni_2P from the International Centre for Diffraction Data (ICDD). The crystallite sizes were calculated from XRD peak broadening using the Scherrer equation. For transmission electron microscopy (TEM) analysis, the unsupported NPs were drop-cast onto continuous carbon-coated copper grids (Ted Pella part no. 01824) from a chloroform suspension, and the carbon supported materials were resuspended in hexanes and drop-cast onto lacey carbon-coated copper grids (Ted Pella part no. 01895). Imaging was performed using a FEI Tecnai ST30 TEM operated at 300 kV, and size distributions were determined by measuring the diameter of > 100 particles using ImageJ software (Schneider et al., 2012). The metal and phosphorus loading of the reduced Ni_2P/C was determined by inductively coupled plasma optical emission spectroscopy (ICP-OES) performed by Galbraith Laboratories (Knoxville, TN).

A potentiostat (VMP3 Workstation, BioLogic Science Instruments, USA) was used to conduct abiotic chronopotentiometry (CP) tests, and two cube reactors (14 mL each) separated by an anion exchange membrane were tested at different set currents (0, 1, 2.5, 5, 7.5, 10, 12.5, and 15 mA each for 20 min). Working electrodes (Ni_2P/C, Ni/C, or Pt/C, projected surface area of 6.5 cm^2) were tested with a platinum mesh counter electrode, and a Ag/AgCl reference electrode (RE-5B, BASi, IN). PBS (50 mM) without nutrients was used as the electrolyte for both chambers, the electrolytes with working electrodes were sparged with high purity nitrogen gas for 5 min prior to the tests. Gas samples were analyzed using a gas chromatograph (Model 8610B, SRI Instruments Inc., USA), and the hydrogen production rate (L-H_2/L-d) was calculated based on the volume of hydrogen gas produced, reactor working volume of both chambers (0.056 L), and the total cycle time (~24 h). To exclude the impact of a low current generation at the end of the 24 h cycle, an average current density ($I_{avg,90}$, A/m^2) was used, which was calculated as the average current for the period of time that 90% of the total charge was transferred (Ivanov et al., 2013), divided by cathode surface area (6.5 cm^2). The average current density over the first 5 h of the cycle ($I_{avg,5h}$) was also calculated from the current generated during the first 5 h to compare current densities in the early stage of the cycle. Cathodic hydrogen recovery (the percent of current recovered as hydrogen, r_{cat}, %) and energy yield (recovered energy as hydrogen compared to the electrical energy input, η_E, %) were calculated as previously described (Logan et al., 2008).

3. Results and discussion

3.1. Ni_2P catalyst characterization

Characterization by XRD of the Ni_2P NPs, Ni_2P/C catalyst, and Ni_2P/C catalyst following reduction at 450 °C confirmed that the materials were hexagonal Ni_2P (PDF 01–089-2742) without any observed crystalline phosphide, oxide, or metallic impurities. Line broadening analysis of the (1 1 1) diffraction peaks gave crystallite sizes of 6.7 nm for Ni_2P NPs, 6.8 nm for Ni_2P/C, and 7.2 nm for reduced Ni_2P/C. Size distribution analysis of TEM images, representative examples of which are shown in Supporting information, gave slightly larger overall particle diameters of 9.5 ± 0.8 nm for Ni_2P NPs, 9.4 ± 0.8 nm for Ni_2P/C, and 9.5 ± 0.7 nm for reduced Ni_2P/C. Both the XRD and TEM characterization indicated that the supporting procedure and thermal reduction did not appreciably alter the crystalline phase or particle size. The composition of the reduced Ni_2P/C catalyst, determined by ICP-OES, was 15.9 wt% Ni and 4.3 wt% P, corresponding to a total Ni and P loading of 20.2 wt%. The slight excess of P (0.14 wt%) relative to the stoichiometry of the Ni_2P phase (20.1 wt% on a Ni-basis) may be due to residual P-species on the surface of the NPs and/or on the support.

3.2. Electrochemical tests at different solution pHs

The HER activity of the Ni_2P/C and Pt/C cathodes was evaluated at different pH values to understand the impact of moving to neutral pH for MECs. The Ni_2P cathode produced more positive electrode potentials at the lower pH (Fig. 1). For example, the Ni_2P/C cathode had a potential of −0.51 V (vs. Ag/AgCl) at pH 2 and −0.90 V (vs. Ag/AgCl) at pH 7 at a set current of 3.8 A/m^2. An acidic pH was more favorable for HER than a neutral pH because a higher proton concentration enhances adsorption of hydrogen atoms (Volmer step) onto the active sites (Conway and Bai, 1986; Marković et al., 1997; Zhou et al., 2017). Similar Ni_2P/C catalysts have been used to produce hydrogen through

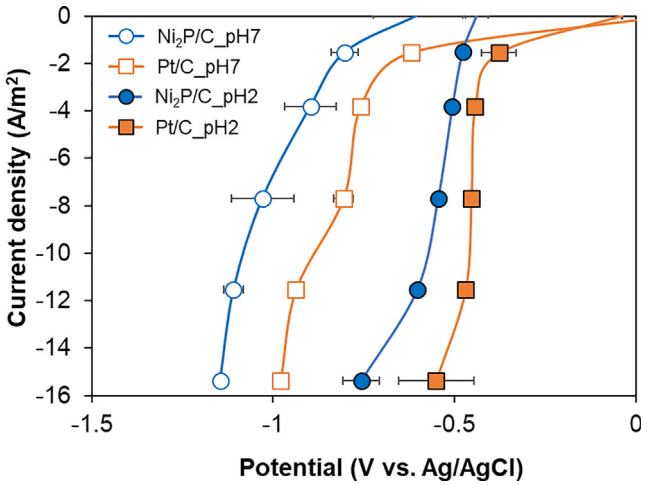

Fig. 1. Chronopotentiometry (CP) test results from Ni_2P/C and Pt/C catalysts at different pHs (pH 2 and pH 7). Error bars indicate the mean ± SD (n = 2), electrode potentials were presented vs. Ag/AgCl.

water electrolysis, but primarily in strongly acidic solutions (e.g., 0.5 M H_2SO_4, pH = 0.3) where they were shown to have catalytic activities comparable to Pt (Popczun et al., 2013). However, at the neutral pHs required for MECs (Gil et al., 2003; He et al., 2008; Nam and Logan, 2012), larger differences have been reported between non-noble metals and Pt in the range of current densities typical for MECs (< 10 A/m^2) (Cai et al., 2016; Hu et al., 2008; Kim et al., 2017). In this study, larger differences in the required potential to achieve a specified current density were also observed for Ni_2P/C and Pt/C under neutral conditions as compared to acidic conditions (0.18 ± 0.04 V difference at pH 7, 0.09 ± 0.02 V difference at pH 2). These observed comparative changes in potential between Ni_2P/C and Pt/C at acidic vs. neutral pH are similar to those observed by others (Zhou et al., 2017).

3.3. Current generation of MECs

The Ni_2P/C, Ni/C, and Pt/C cathodes were tested in MECs for 11 days. The MECs with a Ni_2P/C cathode produced an average current density (over the first 5 h, $I_{avg,5h}$) of 5.7 ± 0.1 A/m^2, which was slightly lower than the MECs with a Pt/C cathode (6.9 ± 0.2 A/m^2), but higher than the MECs with an Ni/C cathode (4.6 ± 0.1 A/m^2) (Fig. 2). Importantly, the Ni_2P loading on the Ni_2P/C cathode (0.5 mg Ni_2P/cm^2) was an order of magnitude lower than the Ni loading on the Ni/C cathode (6 mg Ni/cm^2). This result supports the high HER activity of the Ni_2P catalyst; normalizing the current densities to the mass of catalyst used (A/g-catalyst) gave a normalized current density of 1.14 ± 0.02 A/g-Ni_2P for the Ni_2P/C cathode, which is 14 times higher than the current density of the Ni/C cathode (0.08 ± 0.00 A/g-Ni). The MECs with a Pt/C cathode produced the highest current densities at the beginning of cycle (< 5h), but thereafter they produced lower current densities than Ni_2P/C and Ni/C cathodes, likely due to lower substrate concentrations as shown in Supporting information. Interestingly, while the Ni_2P/C cathode produced higher current densities during the first 5 h of each cycle than the Ni/C cathode, both cathodes exhibited similar current densities for the remainder of each cycle. This observed trend may indicate the rate of H_2 generation is limited by the rate of substrate consumption, not the HER rate of the cathode, at cycle times > 5 h over these two materials.

Average current densities produced by the MECs over the time that 90% of the total charge was transferred ($I_{avg,90}$) were not significantly different (student *t*-test: $p > 0.05$): the Ni_2P/C cathode produced $I_{avg,90}$ = 3.5 ± 0.2 A/m^2, compared to 3.5 ± 0.3 A/m^2 for Pt/C and 3.4 ± 0.2 A/m^2 for Ni/C. The time to reach 90% of coulomb accumulation ($I_{avg,90}$ time) was 17 ± 2 h for the Ni_2P and 14 ± 2 h for the Pt/C (Fig. 2B), which indicated that the Pt/C cathode depleted the substrate sooner than the Ni_2P/C cathode. This result is further supported by the high initial current density for Pt/C as shown in Supporting information.

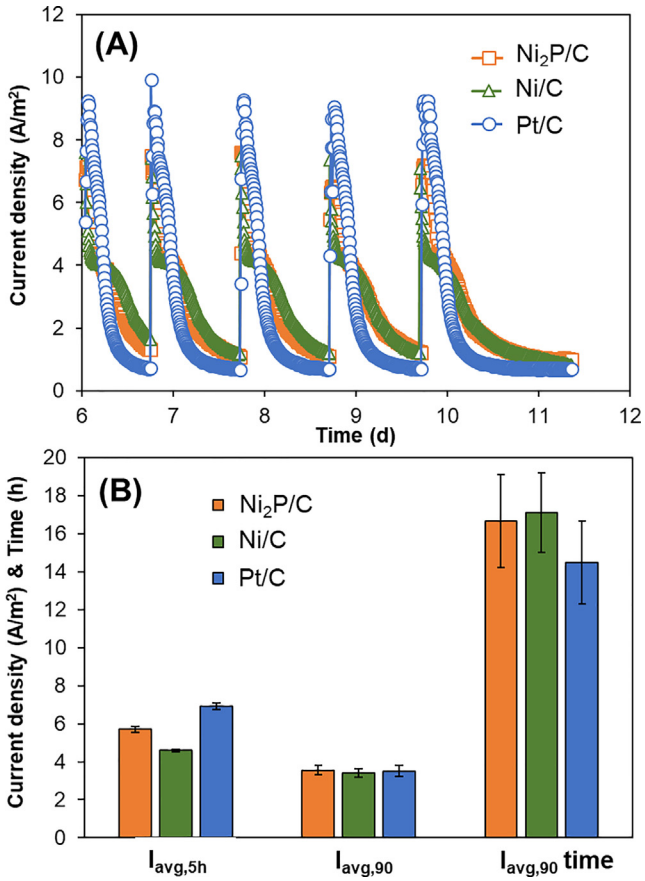

Fig. 2. (A) Current generation of MECs with Ni_2P/C, Ni/C, and Pt/C cathodes over 11 days (0.9 V applied voltage). (B) average current densities over the first 5 h ($I_{avg,5h}$), average current densities over the time that 90% of the total charge transferred ($I_{avg,90}$), and the time to reach 90% coulombs transferred ($I_{avg,90}$ time) for the tested cathodes. Error bars indicate the mean ± SD (n = 4).

Higher $I_{avg,90}$ (3.5 A/m^2) were produced in this study compared to those in a previous study with nickel-adsorbed activated carbon cathodes (2.7 A/m^2), with all test conditions identical except for placement of the cathode (Kim et al., 2018). The higher current here could have also been due to placement of the cathodes against the AEM, instead of placing them in the middle of the chamber, which reduced the electrode distance and the ohmic losses due to the solution resistance (Cario et al., 2019; Rossi et al., 2019).

The Ni_2P/C catalyst was examined over 11 days (including the acclimation phase) and no changes in the performance of the Ni_2P/C catalyst were found during our tests as shown in Supporting Information. The Ni_2P/C catalyst was tested longer than in previous MEC studies where Ni-P cathodes were investigated. In one study, the Ni-P catalyst was only examined over 80 h (3.3 days) with 3 cycles (Li et al., 2017).

3.4. Hydrogen production rates

The hydrogen production rate for MECs with a Ni_2P/C cathode was 0.29 ± 0.04 L-H_2/L-d averaged over a 24 h cycle (Fig. 3). This rate was not significantly different (student *t*-test: $p > 0.05$) than those obtained using Pt/C (0.32 ± 0.03 L-H_2/L-d) or Ni/C (0.29 ± 0.02 L-H_2/L-d) cathodes. While the maximum rates of current production for a Pt/C cathode was higher than that of the other materials examined here

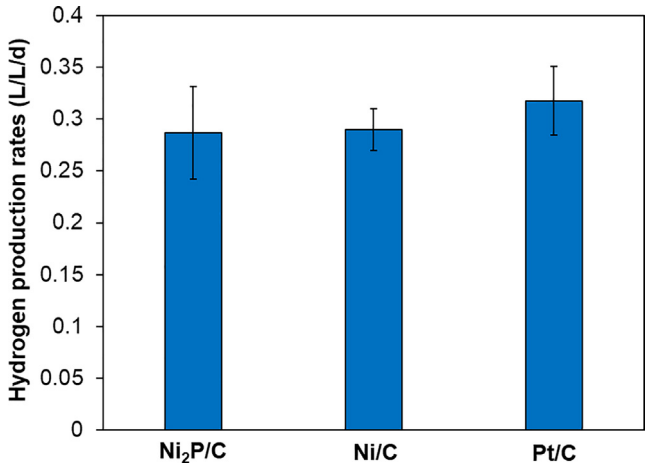

Fig. 3. Hydrogen production rates (L-H_2/L-d) of the MECs over a 24 h cycle with Ni_2P/C, Ni/C, and Pt/C catalyst cathodes (over 11 days, 0.9 V applied voltage). Error bars indicate the mean ± SD (n = 3).

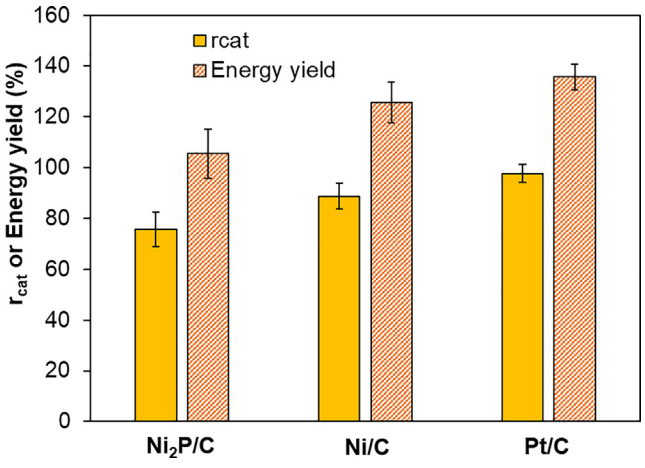

Fig. 4. Cathodic hydrogen recoveries (r_{cat}) and energy yields of the MECs with Ni_2P/C, Ni/C, and Pt/C cathodes (0.9 V applied voltage). Error bars indicate the mean ± SD (n = 4).

(Fig. 2), these differences were not important over the course of the cycle because of the cycle time needed to deplete the substrate. If the cycles had been stopped earlier, for example at the time where 90% of the current was transferred, then the Pt/C cathodes would have had a higher H_2 production rate.

Comparable hydrogen production was obtained for the Ni_2P/C and Pt/C cathodes over the 5 cycles under neutral pH. Furthermore, the Ni_2P/C cathode (catalyst loading of 0.5 mg-Ni_2P/cm^2) had comparable hydrogen production to the Ni/C cathode (6 mg-Ni/cm^2), even with 12 times less catalyst mass used. These excellent results using the Ni_2P/C catalyst were likely due to the function of the P heteroatom, as it can electrostatically attract protons to the active sites and reduce hydrogen bonding energy (Liu and Rodriguez, 2005).

The hydrogen production rates obtained here with the synthetic fermentation effluent were lower than those produced when acetate was used as the sole substrate (Rozendal et al., 2007; Zikmund et al., 2018). The synthetic fermentation effluent contained a high concentration of protein (0.32 g/L), and it has been demonstrated that hydrogen production using protein is less than that obtained using acetate as current cannot be generated directly from oxidation of the protein (Lu et al., 2010; Nam et al., 2014). The hydrogen production rates are also reduced when a membrane is used in the system due to the increased internal resistance (Cai et al., 2016; Lu et al., 2016). However, the use of two chambers versus a single chamber has the advantage of reducing the loss of hydrogen by methane production, or hydrogen crossover from the cathode to the anode (Cusick et al., 2011). In a previous study using a Ni_5P_4-NiP_2 nanosheet cathode in a single chamber MEC with acetate as the substrate, slightly more hydrogen gas was produced per day (20 mL-H_2 per day) than this study (15 mL-H_2/day) (Cai et al., 2018), but it is difficult to directly compare these rates due to the different reactor configurations and substrates.

3.5. Energy efficiency and cathodic H_2 recovery

All MECs had energy efficiencies relative to the electrical power added that were higher than 100%, based on the amount of hydrogen gas recovered over the cycle (Fig. 4). That is, energy content in the produced hydrogen (−237.1 kJ/mole-H_2, Gibbs free energy) was higher in all MECs than energy input (0.9 V applied potential for the 24 h cycle) due to the inherent energy content of the synthetic fermentation effluent that is not accounted for in these efficiency calculations. The percent of the measured current recovered as hydrogen using the Ni_2P cathode was r_{cat} = 76 ± 7% over a 24 h cycle, which was significantly lower ($p < 0.05$) than that obtained using Pt/C (98 ± 4%) or Ni/C (89 ± 5%) cathodes (Fig. 4). Although the amount of recovered hydrogen gas with the Ni_2P cathode was similar to the other two cathodes, the Ni_2P/C produced more coulombs (152 ± 14C) from the substrate than the Pt/C (131 ± 11C) cathode over a 24 h cycle. This higher quantity of coulombs produced was due to a higher current density (> 1 A/m^2) that was maintained until the end of each cycle (Fig. 2A). The reason for this higher current density is not known, but it is possible that there was an unidentified parasitic reaction at the cathode, which was not related to HER.

4. Conclusions

Hexagonal phase-pure Ni_2P nanoparticles were synthesized, dispersed on carbon, and evaluated in an MEC as an alternative HER catalyst in a neutral pH electrolyte. Based on hydrogen recoveries over a 24 h cycle, the MEC with the Ni_2P/C cathode had an average hydrogen production rate (0.29 ± 0.04 L-H_2/L-d) and current density that were comparable to those of Pt/C and Ni/C. The use of Ni_2P nanoparticles as an alternative catalyst in MECs is therefore feasible in terms of hydrogen production and the stability compared to other forms of nickel, albeit further testing is required to demonstrate performance over extended cycles.

Acknowledgements

This work was authored in part by the National Renewable Energy Laboratory (NREL), operated by Alliance for Sustainable Energy, LLC, for the U.S. Department of Energy (DOE) under Contract No. DE-AC36-08GO28308. This work was supported by the Laboratory Directed Research and Development (LDRD) Program at NREL. Funding was also provided by the U.S. DOE Office of Energy Efficiency and Renewable Energy, and Bioenergy Technologies Office as part of the ChemCatBio Consortium, an Energy Materials Network Consortium. The views expressed in the article do not necessarily represent the views of the DOE or the U.S. Government. This work was also supported by funds provided by the NREL through the Department of Energy (DOE) CPS Project #21263. The U.S. Government retains and the publisher, by accepting the article for publication, acknowledges that the U.S. Government retains a non-exclusive, paid-up, irrevocable, worldwide license to publish or reproduce the published form of this manuscript, or allow others to do so, for U.S. Government purposes.

Appendix A. Supplementary data

Supplementary data to this article can be found online at https://

doi.org/10.1016/j.biortech.2019.122067.

References

Cai, W., Liu, W., Han, J., Wang, A., 2016. Enhanced hydrogen production in microbial electrolysis cell with 3D self-assembly nickel foam-graphene cathode. Biosens. Bioelectron. 80, 118–122.

Cai, W., Liu, W., Sun, H., Li, J., Yang, L., Liu, M., Zhao, S., Wang, A., 2018. Ni_5P_4-NiP_2 nanosheet matrix enhances electron-transfer kinetics for hydrogen recovery in microbial electrolysis cells. Appl. Energ. 209, 56–64.

Call, D.F., Merrill, M.D., Logan, B.E., 2009. High surface area stainless steel brushes as cathodes in microbial electrolysis cells. Environ. Sci. Technol. 43 (6), 2179–2183.

Cario, B.P., Rossi, R., Kim, K.-Y., Logan, B.E., 2019. Applying the electrode potential slope method as a tool to quantitatively evaluate the performance of individual microbial electrolysis cell components. Bioresour. Technol. 287, 121418.

Conway, B.E., Bai, L., 1986. Determination of adsorption of OPD H species in the cathodic hydrogen evolution reaction at Pt in relation to electrocatalysis. J. Electroanal. Chem. 198 (1), 149–175.

Cusick, R.D., Bryan, B., Parker, D.S., Merrill, M.D., Mehanna, M., Kiely, P.D., Liu, G., Logan, B.E., 2011. Performance of a pilot-scale continuous flow microbial electrolysis cell fed winery wastewater. Appl. Microbiol. Biotechnol. 89 (6), 2053–2063.

Feng, L., Vrubel, H., Bensimon, M., Hu, X., 2014. Easily-prepared dinickel phosphide (Ni_2P) nanoparticles as an efficient and robust electrocatalyst for hydrogen evolution. PCCP 16 (13), 5917–5921.

Feng, Y., Yang, Q., Wang, X., Logan, B.E., 2010. Treatment of graphite fiber brush anodes for improving power generation in air-cathode microbial fuel cells. J. Power Sources 195 (7), 1841–1844.

Gil, G.-C., Chang, I.-S., Kim, B.H., Kim, M., Jang, J.-K., Park, H.S., Kim, H.J., 2003. Operational parameters affecting the performannce of a mediator-less microbial fuel cell. Biosens. Bioelectron. 18 (4), 327–334.

Habas, S.E., Baddour, F.G., Ruddy, D.A., Nash, C.P., Wang, J., Pan, M., Hensley, J.E., Schaidle, J.A., 2015. A facile molecular precursor route to metal phosphide nanoparticles and their evaluation as hydrodeoxygenation catalysts. Chem. Mater. 27 (22), 7580–7592.

Han, A., Jin, S., Chen, H., Ji, H., Sun, Z., Du, P., 2015. A robust hydrogen evolution catalyst based on crystalline nickel phosphide nanoflakes on three-dimensional graphene/nickel foam: high performance for electrocatalytic hydrogen production from pH 0–14. J. Mater. Chem. A 3 (5), 1941–1946.

He, Z., Huang, Y., Manohar, A.K., Mansfeld, F., 2008. Effect of electrolyte pH on the rate of the anodic and cathodic reactions in an air-cathode microbial fuel cell. Bioelectrochemistry 74 (1), 78–82.

Hrapovic, S., Manuel, M.-F., Luong, J., Guiot, S., Tartakovsky, B., 2010. Electrodeposition of nickel particles on a gas diffusion cathode for hydrogen production in a microbial electrolysis cell. Int. J. Hydrogen Energy 35 (14), 7313–7320.

Hu, H., Fan, Y., Liu, H., 2008. Hydrogen production using single-chamber membrane-free microbial electrolysis cells. Water Res. 42 (15), 4172–4178.

Ivanov, I., Ren, L., Siegert, M., Logan, B.E., 2013. A quantitative method to evaluate microbial electrolysis cell effectiveness for energy recovery and wastewater treatment. Int. J. Hydrogen Energy 38 (30), 13135–13142.

Jeremiasse, A.W., Hamelers, H.V., Saakes, M., Buisman, C.J., 2010. Ni foam cathode enables high volumetric H_2 production in a microbial electrolysis cell. Int. J. Hydrogen Energy 35 (23), 12716–12723.

Kim, K.-Y., Logan, B.E., 2019. Nickel powder blended activated carbon cathodes for hydrogen production in microbial electrolysis cells. Int. J. Hydrogen Energy 44 (26), 13169–13174.

Kim, K.-Y., Yang, W., Logan, B.E., 2018. Regenerable Nickel-Functionalized Activated Carbon Cathodes Enhanced by Metal Adsorption to Improve Hydrogen Production in Microbial Electrolysis Cells. Environ. Sci. Technol. 52 (12), 7131–7137.

Kim, K.-Y., Zikmund, E., Logan, B.E., 2017. Impact of catholyte recirculation on different 3-dimensional stainless steel cathodes in microbial electrolysis cells. Int. J. Hydrogen Energy 42 (50), 29708–29715.

Laursen, A.B., Patraju, K.R., Whitaker, M.J., Retuerto, M., Sarkar, T., Yao, N., Ramanujachary, K.V., Greenblatt, M., Dismukes, G.C., 2015. Nanocrystalline Ni_5P_4: a hydrogen evolution electrocatalyst of exceptional efficiency in both alkaline and acidic media. Energy Environ. Sci. 8 (3), 1027–1034.

Li, F., Liu, W., Sun, Y., Ding, W., Cheng, S., 2017. Enhancing hydrogen production with Ni–P coated nickel foam as cathode catalyst in single chamber microbial electrolysis cells. Int. J. Hydrogen Energy 42 (6), 3641–3646.

Liu, P., Rodriguez, J.A., 2005. Catalysts for hydrogen evolution from the [NiFe] hydrogenase to the Ni_2P(001) surface: The importance of ensemble effect. J. Am. Chem. Soc. 127 (42), 14871–14878.

Logan, B.E., Call, D., Cheng, S., Hamelers, H.V., Sleutels, T.H., Jeremiasse, A.W., Rozendal, R.A., 2008. Microbial electrolysis cells for high yield hydrogen gas production from organic matter. Environ. Sci. Technol. 42 (23), 8630–8640.

Lu, L., Hou, D., Fang, Y., Huang, Y., Ren, Z.J., 2016. Nickel based catalysts for highly efficient H_2 evolution from wastewater in microbial electrolysis cells. Electrochim. Acta 206, 381–387.

Lu, L., Ren, Z.J., 2016. Microbial electrolysis cells for waste biorefinery: A state of the art review. Bioresour. Technol. 215, 254–264.

Lu, L., Xing, D., Xie, T., Ren, N., Logan, B.E., 2010. Hydrogen production from proteins via electrohydrogenesis in microbial electrolysis cells. Biosens. Bioelectron. 25 (12), 2690–2695.

Marković, N.M., Grgur, B.N., Ross, P.N., 1997. Temperature-dependent hydrogen electrochemistry on platinum low-index single-crystal surfaces in acid solutions. J. Phys. Chem. B 101 (27), 5405–5413.

Nam, J.-Y., Logan, B.E., 2012. Optimization of catholyte concentration and anolyte pHs in two chamber microbial electrolysis cells. Int. J. Hydrogen Energy 37 (24), 18622–18628.

Nam, J.-Y., Yates, M.D., Zaybak, Z., Logan, B.E., 2014. Examination of protein degradation in continuous flow, microbial electrolysis cells treating fermentation wastewater. Bioresour. Technol. 171, 182–186.

Nørskov, J.K., Bligaard, T., Logadottir, A., Kitchin, J., Chen, J.G., Pandelov, S., Stimming, U., 2005. Trends in the exchange current for hydrogen evolution. J. Electrochem. Soc. 152 (3), J23–J26.

Pan, Y., Liu, Y., Zhao, J., Yang, K., Liang, J., Liu, D., Hu, W., Liu, D., Liu, Y., Liu, C., 2015. Monodispersed nickel phosphide nanocrystals with different phases: synthesis, characterization and electrocatalytic properties for hydrogen evolution. J. Mater. Chem. A 3 (4), 1656–1665.

Popczun, E.J., McKone, J.R., Read, C.G., Biacchi, A.J., Wiltrout, A.M., Lewis, N.S., Schaak, R.E., 2013. Nanostructured nickel phosphide as an electrocatalyst for the hydrogen evolution reaction. J. Am. Chem. Soc. 135 (25), 9267–9270.

Ribot-Llobet, E., Nam, J.-Y., Tokash, J.C., Guisasola, A., Logan, B.E., 2013. Assessment of four different cathode materials at different initial pHs using unbuffered catholytes in microbial electrolysis cells. Int. J. Hydrogen Energy 38 (7), 2951–2956.

Rossi, R., Cario, B.P., Santoro, C., Yang, W., Saikaly, P.E., Logan, B.E., 2019. Evaluation of electrode and solution area-based resistances enables quantitative comparisons of factors impacting microbial fuel cell performance. Environ. Sci. Technol. 53 (7), 3977–3986.

Rozendal, R.A., Hamelers, H.V., Euverink, G.J., Metz, S.J., Buisman, C.J., 2006. Principle and perspectives of hydrogen production through biocatalyzed electrolysis. Int. J. Hydrogen Energy 31 (12), 1632–1640.

Rozendal, R.A., Hamelers, H.V.M., Rabaey, K., Keller, J., Buisman, C.J.N., 2008. Towards practical implementation of bioelectrochemical wastewater treatment. Trends Biotechnol. 26 (8), 450–459.

Rozendal, R.A., Jeremiasse, A.W., Hamelers, H.V., Buisman, C.J., 2007. Hydrogen production with a microbial biocathode. Environ. Sci. Technol. 42 (2), 629–634.

Schneider, C.A., Rasband, W.S., Eliceiri, K.W., 2012. NIH Image to ImageJ: 25 years of image analysis. Nat. Methods 9, 671.

Selembo, P.A., Merrill, M.D., Logan, B.E., 2010. Hydrogen production with nickel powder cathode catalysts in microbial electrolysis cells. Int. J. Hydrogen Energy 35 (2), 428–437.

Seo, B., Baek, D.S., Sa, Y.J., Joo, S.H., 2016. Shape effects of nickel phosphide nanocrystals on hydrogen evolution reaction. CrystEngComm 18 (32), 6083–6089.

Shi, Y., Xu, Y., Zhuo, S., Zhang, J., Zhang, B., 2015. Ni_2P nanosheets/Ni Foam composite electrode for long-lived and pH-tolerable electrochemical hydrogen generation. ACS Appl. Mater. Interfaces 7 (4), 2376–2384.

Shi, Y., Zhang, B., 2016. Recent advances in transition metal phosphide nanomaterials: synthesis and applications in hydrogen evolution reaction. Chem. Soc. Rev. 45 (6), 1529–1541.

Sun, Y., Hang, L., Shen, Q., Zhang, T., Li, H., Zhang, X., Lyu, X., Li, Y., 2017. Mo doped Ni_2P nanowire arrays: an efficient electrocatalyst for the hydrogen evolution reaction with enhanced activity at all pH values. Nanoscale 9 (43), 16674–16679.

Tokash, J., Logan, B., 2011. Electrochemical evaluation of molybdenum disulfide as a catalyst for hydrogen evolution in microbial electrolysis cells. Int. J. Hydrogen Energy 36 (16), 9439–9445.

Wu, M.-Y., Da, P.-F., Zhang, T., Mao, J., Liu, H., Ling, T., 2018. Designing hybrid NiP_2/NiO nanorod arrays for efficient alkaline hydrogen evolution. ACS Appl. Mater. Interfaces 10 (21), 17896–17902.

Xiao, P., Chen, W., Wang, X., 2015. A review of phosphide-based materials for electrocatalytic hydrogen evolution. Adv. Energy Mater. 5 (24), 1500985.

Zhang, R., Wang, X., Yu, S., Wen, T., Zhu, X., Yang, F., Sun, X., Wang, X., Hu, W., 2017. Ternary $NiCo_2Px$ nanowires as pH-universal electrocatalysts for highly efficient hydrogen evolution reaction. Adv. Mater. 29 (9), 1605502.

Zhou, M., Kang, Y., Huang, K., Shi, Z., Xie, R., Yang, W., 2016. Ultra-small nickel phosphide nanoparticles as a high-performance electrocatalyst for the hydrogen evolution reaction. RSC Adv. 6 (78), 74895–74902.

Zhou, Z., Wei, L., Wang, Y., Karahan, H.E., Chen, Z., Lei, Y., Chen, X., Zhai, S., Liao, X., Chen, Y., 2017. Hydrogen evolution reaction activity of nickel phosphide is highly sensitive to electrolyte pH. J. Mater. Chem. A 5 (38), 20390–20397.

Zikmund, E., Kim, K.-Y., Logan, B.E., 2018. Hydrogen production rates with closely-spaced felt anodes and cathodes compared to brush anodes in two-chamber microbial electrolysis cells. Int. J. Hydrogen Energy 43 (20), 9599–9606.